



**Stably Transfected Cell Line - Product Data Sheet**  
**hP2X7-HEK**  
**Catalog Number CT6190**

**Related Services and Products**

FLIPR® screening services

Additional information available at [www.chantest.com](http://www.chantest.com)

**Contact Information**

ChanTest Corporation

14656 Neo Parkway

Cleveland OH 44128

Tel: (216) 584-0590

Fax: (216) 584-0591

## Table of Contents

1	Cell Line Description.....	3
1.1	Background.....	3
1.2	Pore-forming subunit identifier: hP2X7 .....	3
1.3	Sequence Information .....	3
1.4	Expression System .....	3
1.5	Product Format.....	3
1.6	Mycoplasma Status: Negative.....	3
1.7	Cell Line Stability .....	3
2	Validated Test Platforms.....	3
2.1	QPatch™ .....	4
2.1.1	Throughput Capability in QPatch™ .....	4
2.1.2	Representative QPatch™ Data .....	5
2.2	FLIPR® Representative Data .....	8
2.2.1	Bz-ATP activation of P2X7 .....	8
2.2.2	Effects of antagonists on P2X7.....	9
3	References.....	11

## 1 Cell Line Description

### 1.1 Background

P2X7 is an ionotropic purinergic receptor that forms a cation-selective channel. Expressed in lymphocytes and microglia, P2X7 is a potential therapeutic target in treatment of osteoporosis, pain, and immune diseases.

### 1.2 Pore-forming subunit identifier: hP2X7

Class: Ionotropic purinergic receptor  
Species: Human  
Gene name: P2RX7

### 1.3 Sequence Information

The cDNA sequence of the P2RX7 gene used to create this cell line was confirmed prior to transfection. The amino acid sequence encoded by the transfected cDNA is identical to the translated sequence for GenBank accession number NM\_002562.4.

### 1.4 Expression System

HEK293 (human embryonic kidney) cells, tetracycline-inducible expression.

### 1.5 Product Format

Cryopreserved cells,  $2 \times 10^6$  cells/vial.

### 1.6 Mycoplasma Status: Negative

The absence of mycoplasma species in this cell line was confirmed with the MycoAlert Kit (Lonza Rockland, Inc.).

### 1.7 Cell Line Stability

Channel expression has been shown to be stable for at least 28 passages.

## 2 Validated Test Platforms

Electrophysiological and pharmacological verification of the functional properties of the cloned channels was assessed in the following test platforms:

QPatch™ (Sophion Bioscience)  
FLIPR® (MDS-AT)

## 2.1 QPatch™

### 2.1.1 Throughput Capability in QPatch™

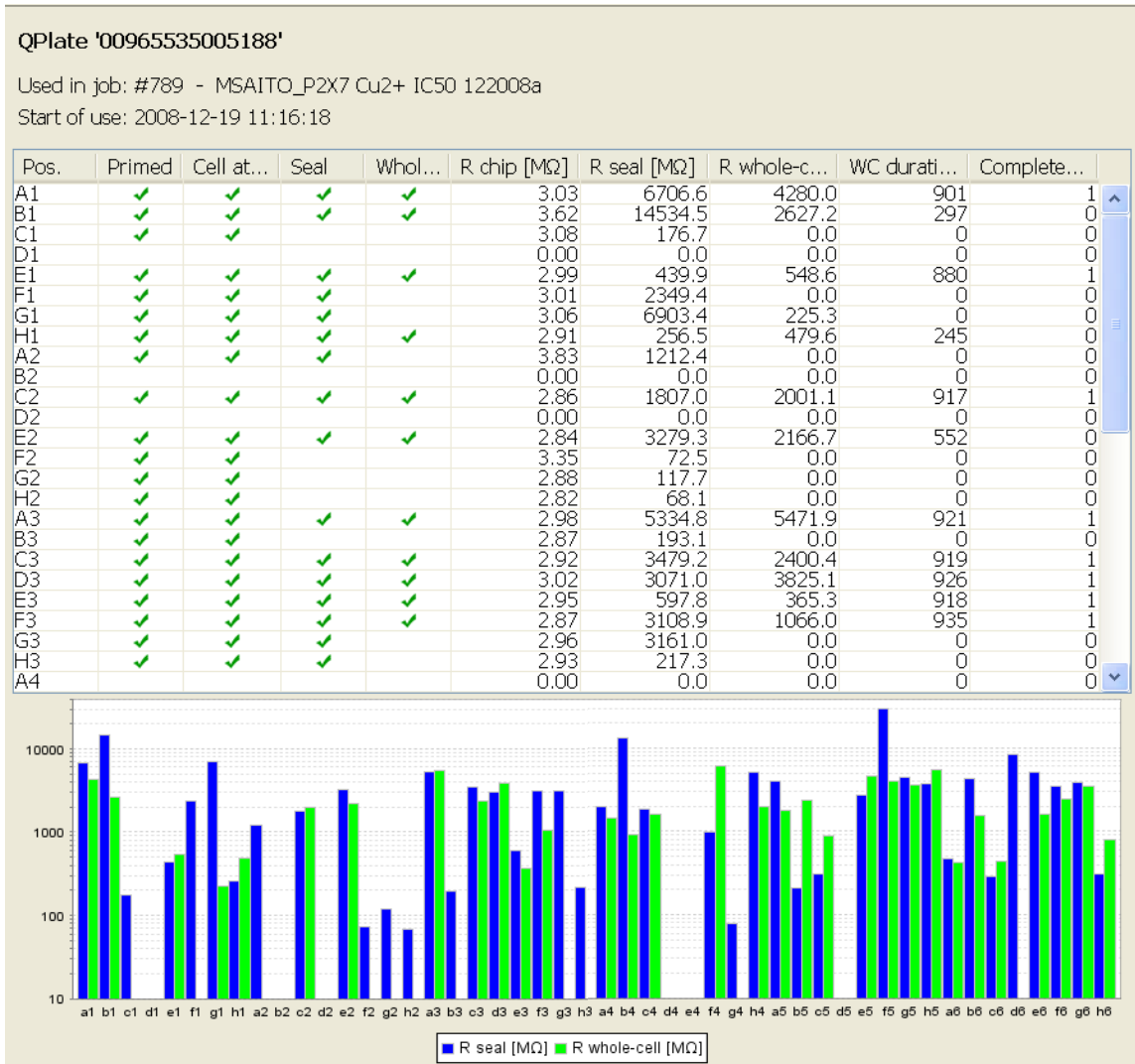


**Figure 1. QPatch™ Screen Capture**

Throughput capability depends upon many factors which may result in success rate variability. In this example, 16 seals were formed of a possible 24; whole-cell configuration was achieved in 11 cells.

### 2.1.2 Representative QPatch™ Data

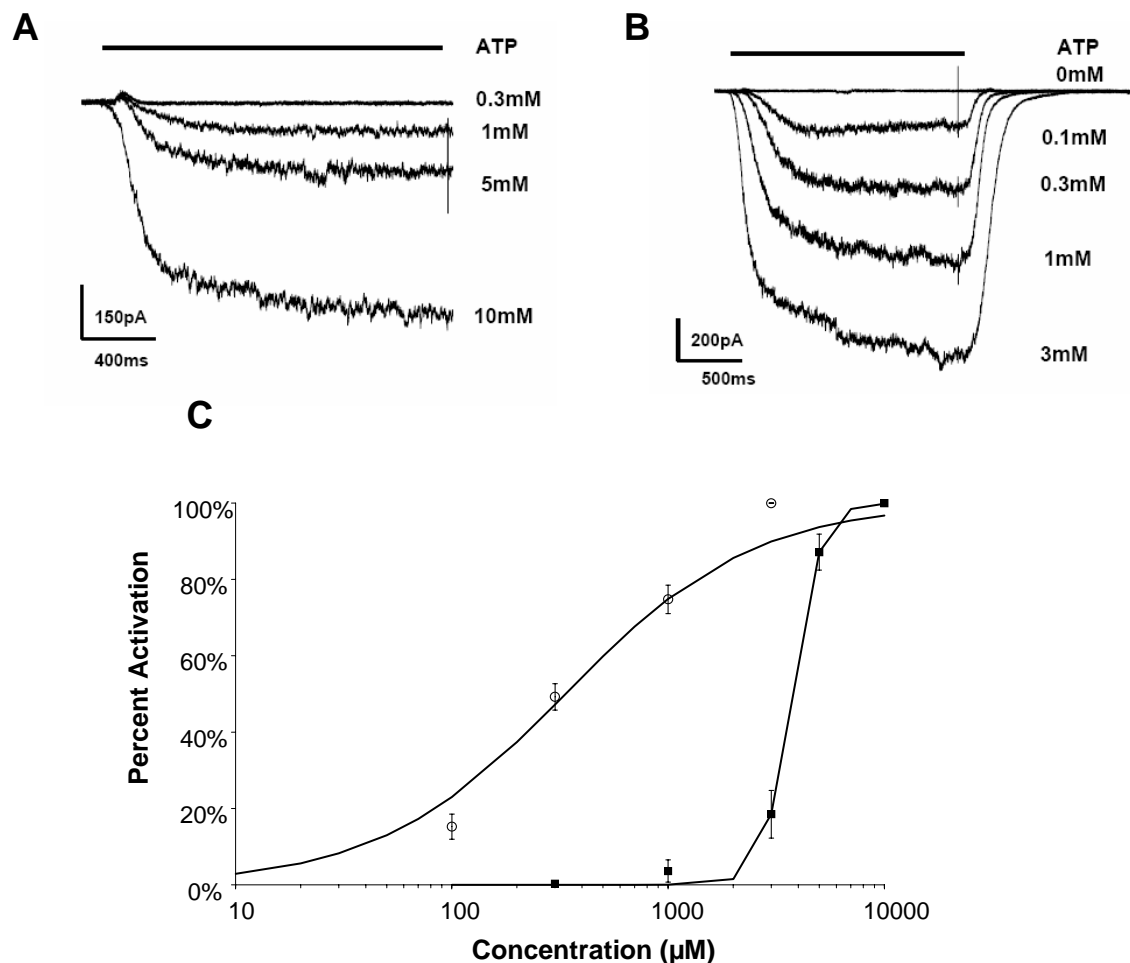


**Figure 2. ATP activation of P2X7 in QPatch™**

**A:** Inward currents evoked by application of increasing concentrations of ATP in assay buffer (HBPS). Holding potential -60 mV. **B:** ATP-evoked currents in divalent cation-free (DVF) HBPS showed increased ATP sensitivity.

**C:** Concentration- response relationships in the presence ( $EC_{50} = 3.75$  mM,  $n = 3$  cells/concentration, filled squares) and absence ( $EC_{50} = 339.6$   $\mu\text{M}$ ,  $n = 10$ , open circles) of divalent cations.

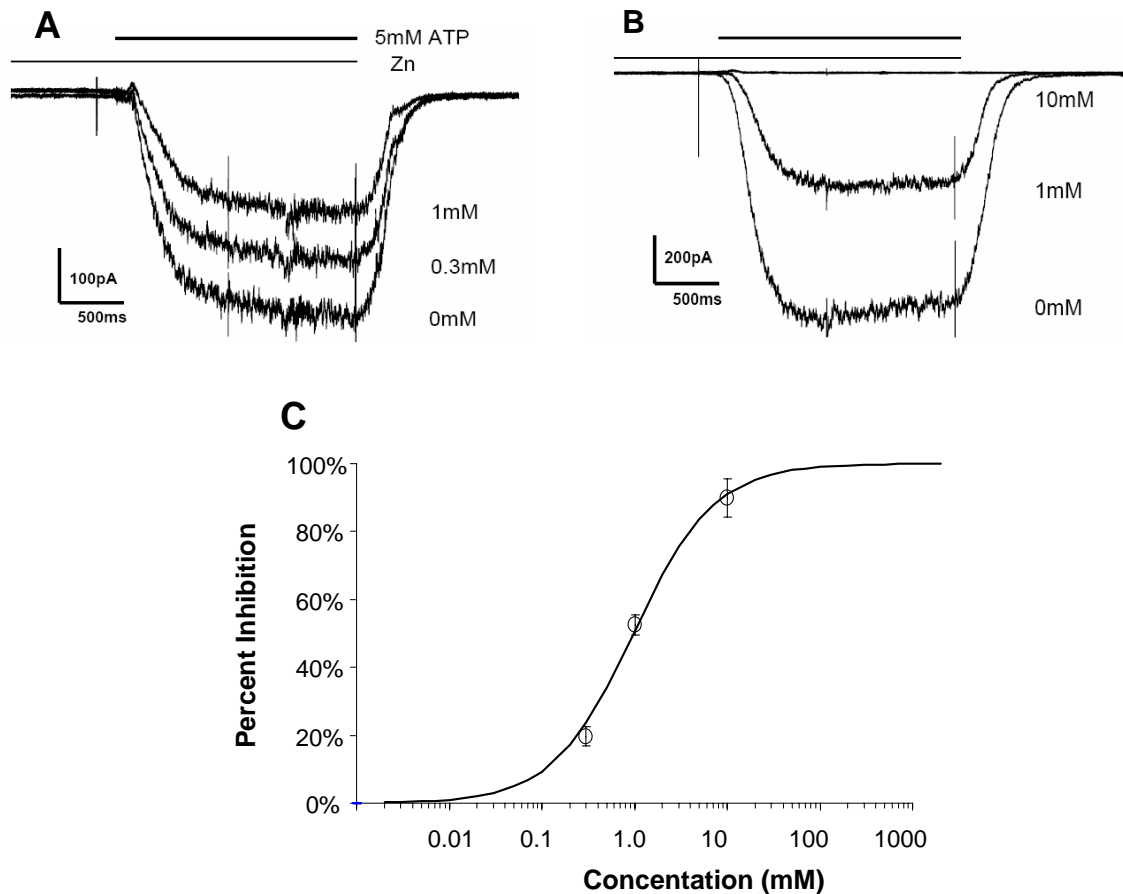


**Figure 3. Zn<sup>2+</sup> inhibition of ATP-activated P2X7 currents**

**A - B:** Current traces evoked by 5 mM ATP in the presence of increasing concentrations of Zn<sup>2+</sup>, holding potential -60 mV. Zn<sup>2+</sup> was applied to the cells before the application of ATP (horizontal bars above the current traces). Recordings were obtained in standard divalent HBPS. **C:** Zn<sup>2+</sup> concentration-response relationship. Mean ± SEM, n = 7 - 15 cells/concentration. IC<sub>50</sub> = 0.971 mM.

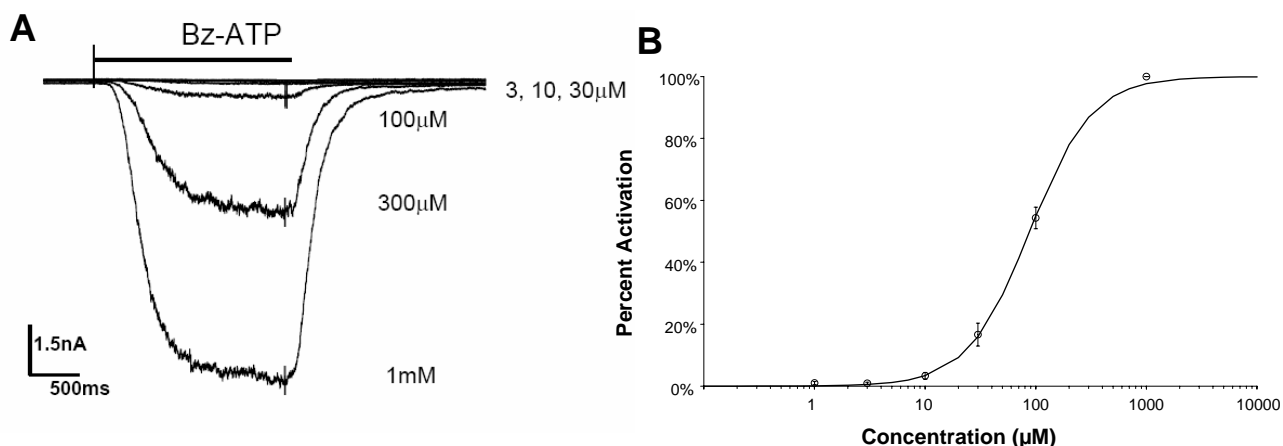


**Figure 4. Bz-ATP activation of P2X7**

**A:** Inward current traces evoked by increasing Bz-ATP concentrations (1, 3, 10, 30, 100, and 1000 μM). Horizontal bar indicates Bz-ATP application. Recordings obtained in in  $Mg^{2+}$ -free HBPS. **B:** Bz-ATP concentration-response relationship. Mean  $\pm$  SEM,  $n = 11$  cells/concentrations.  $EC_{50} = 87.9 \mu M$ .

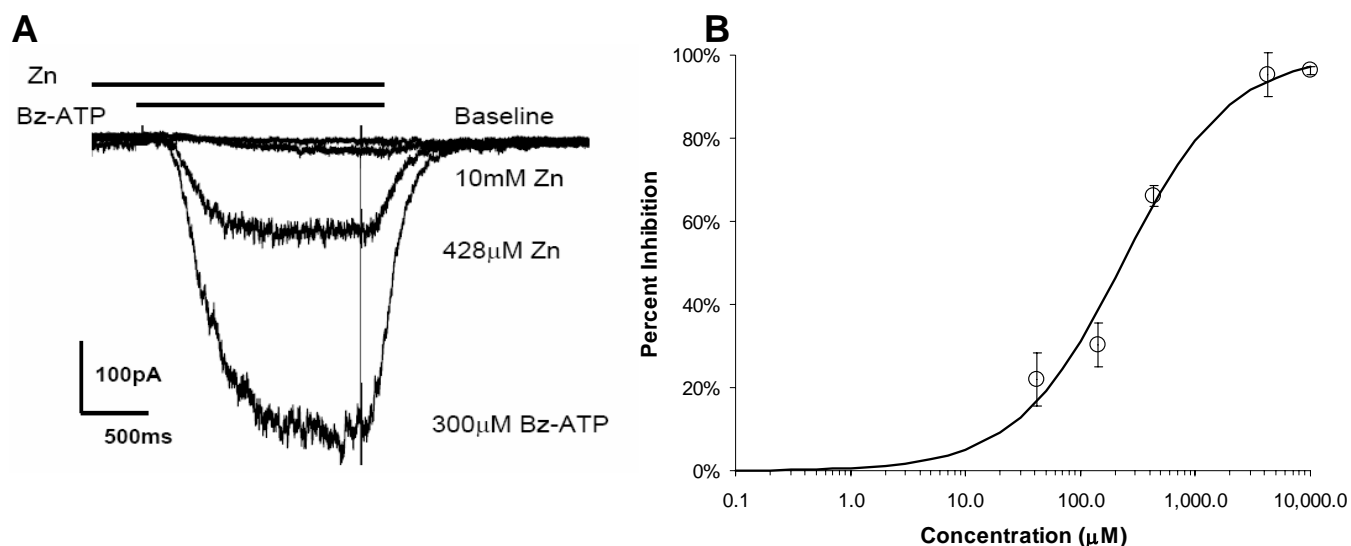


**Figure 5.  $Zn^{2+}$  inhibition of Bz-ATP-induced current**

**A:** Currents evoked by 300 μM Bz-ATP before and after  $Zn^{2+}$  application at 0.428 or 10 mM. on currents recorded in the presence of 300 μM Bz-ATP. Recordings obtained in  $Mg^{2+}$ -free HBPS. **B:** Concentration-response relationship Mean  $\pm$  SEM,  $n = 3 - 6$  cells/concentration.  $IC_{50} = 234 \mu M$ .

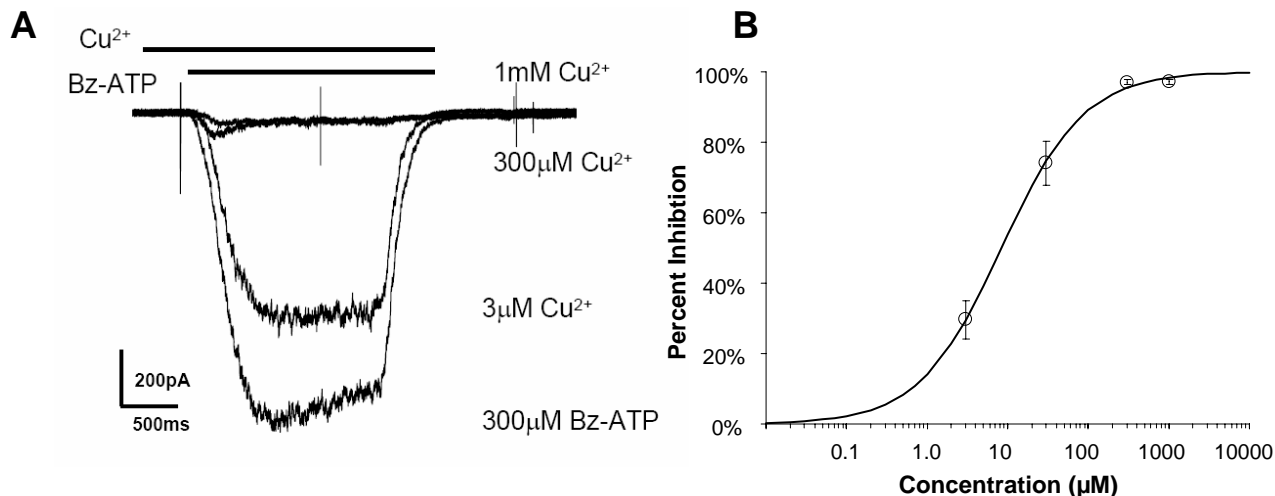


**Figure 6.  $\text{Cu}^{2+}$  inhibition of Bz-ATP induced current**

**A:** Current traces evoked by 300  $\mu\text{M}$  Bz-ATP before and after application of increasing  $\text{Cu}^{2+}$  concentrations (3, 300, and 1000  $\mu\text{M}$ ). Recordings obtained in  $\text{Mg}^{2+}$ -free HBPS.

**B:** Concentration-response relationship. Mean  $\pm$  SEM, n = 7 - 12 cells/concentration.  $\text{IC}_{50} = 8.37\mu\text{M}$ .

## 2.2 FLIPR<sup>®</sup> Representative Data

### 2.2.1 Bz-ATP activation of P2X7

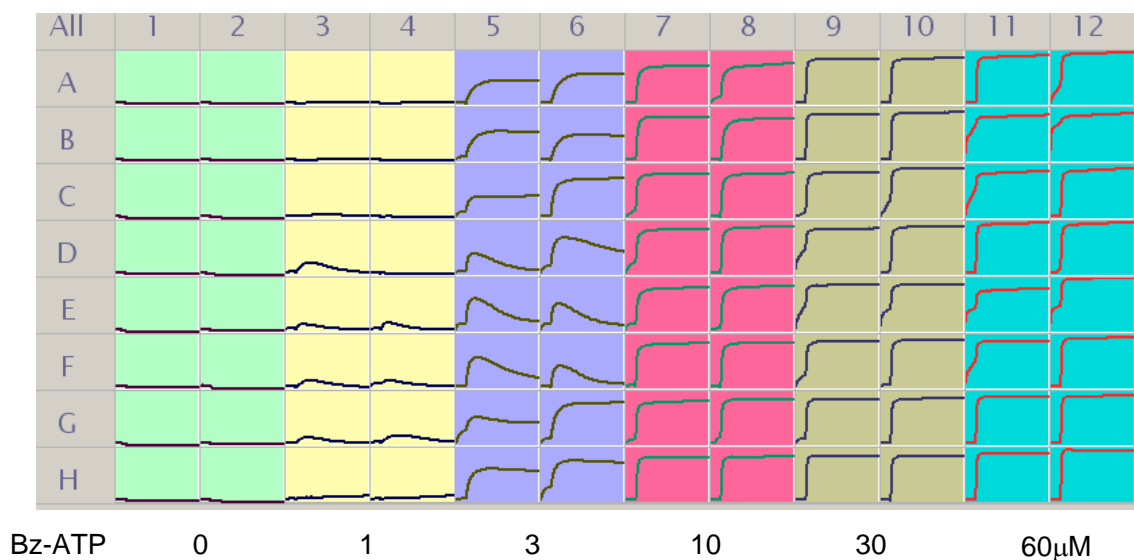


**Figure 7. Bz-ATP activation of P2X7 in FLIPR<sup>®</sup>**

Bz-ATP evoked a concentration-dependent increase in  $[\text{Ca}^{2+}]_i$  in hP2X7-HEK cells.

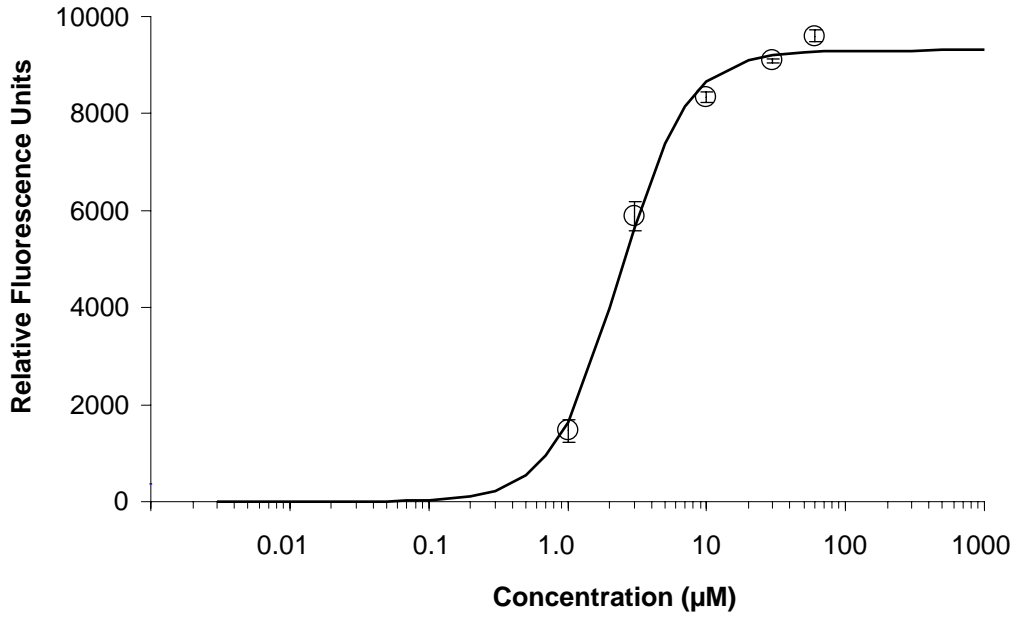


**Figure 8. BzATP concentration-response relationship.**  
Mean  $\pm$  SEM, n = 16 replicates/concentration. EC<sub>50</sub> = 2.4  $\mu$ M.

### 2.2.2 Effects of antagonists on P2X7

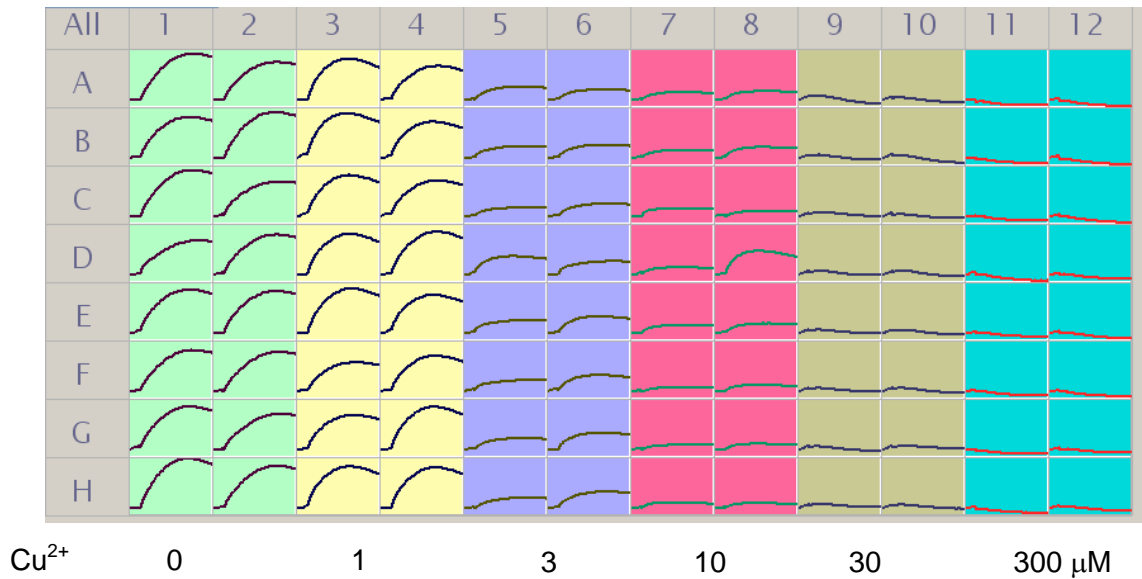


**Figure 9. Concentration-dependent block P2X7 by Cu<sup>2+</sup>.**  
Bz-ATP (30  $\mu$ M)-induced [Ca<sup>2+</sup>]<sub>i</sub> signals in the presence of increasing concentrations of Cu<sup>2+</sup>.

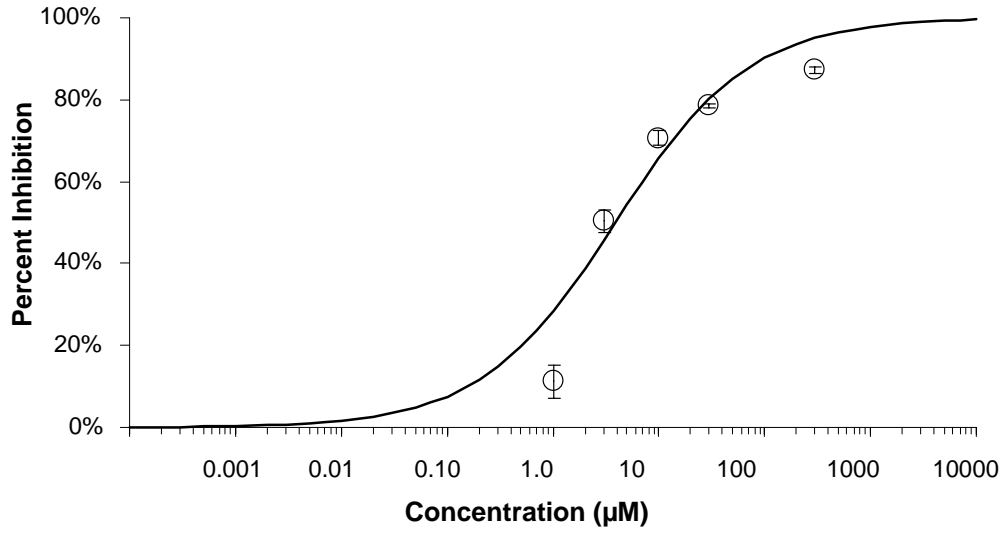


**Figure 10.  $\text{Cu}^{2+}$  concentration-response relationship.**  
Inhibition of BzATP (30  $\mu\text{M}$ )-induced  $[\text{Ca}^{2+}]_i$  signals. Mean  $\pm$  SEM, n = 5 - 16 replicates/concentration.  $\text{IC}_{50}$  = 3.9  $\mu\text{M}$ .

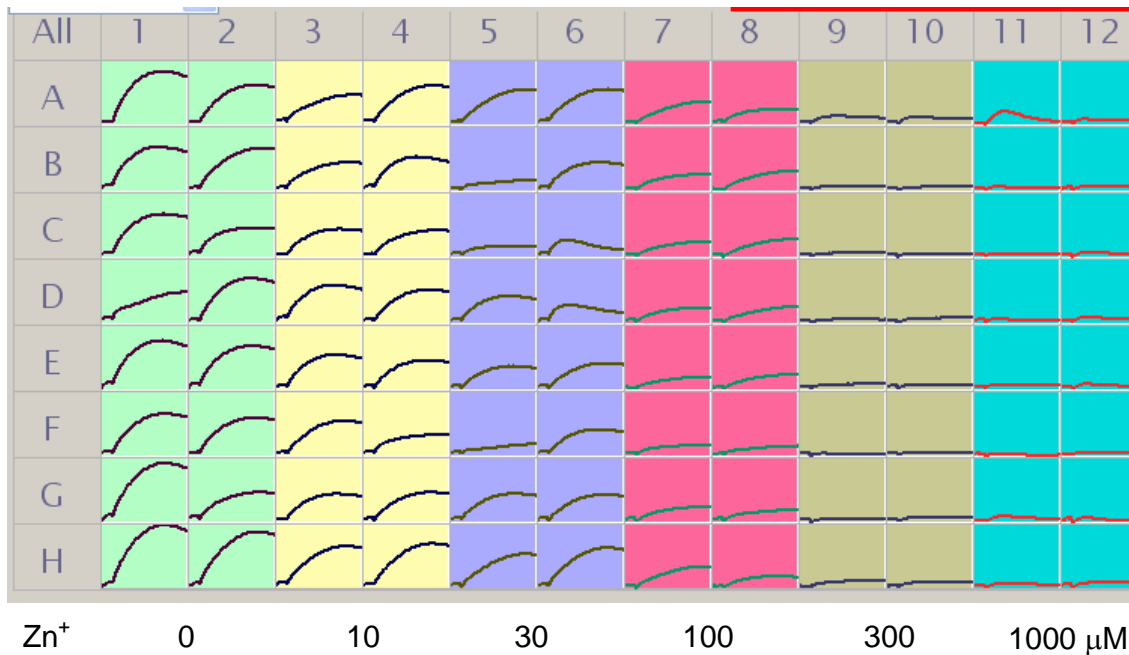


**Figure 11.  $\text{Zn}^{2+}$  concentration-dependent inhibition of P2X7**  
Bz-ATP (30  $\mu\text{M}$ )-induced  $[\text{Ca}^{2+}]_i$  signals in the presence of increasing concentrations of  $\text{Zn}^{2+}$ .

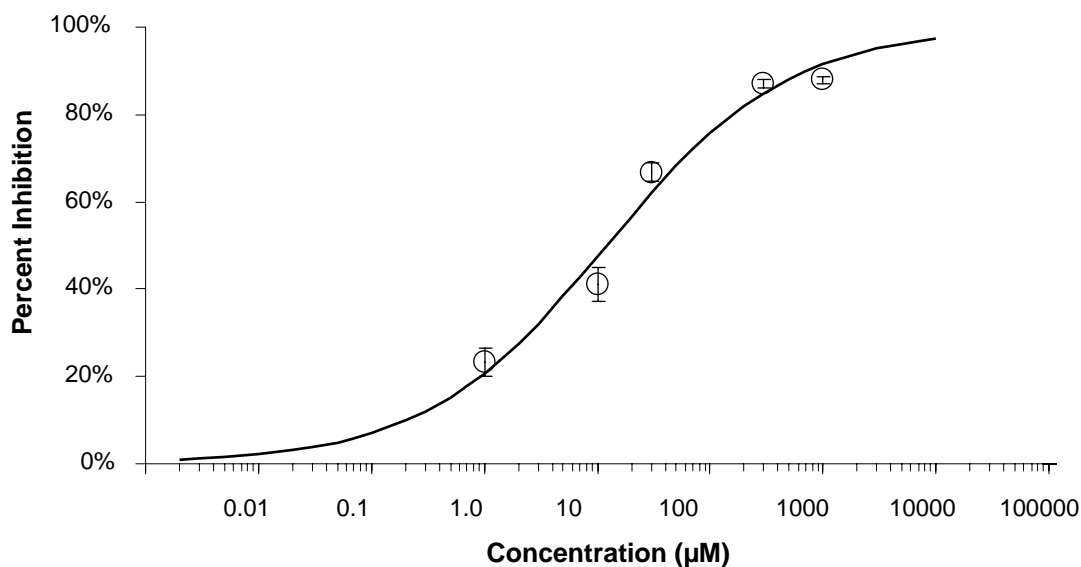


**Figure 12. Zn<sup>2+</sup> concentration-response relationship.**  
Inhibition of Bz-ATP (30 µM) -induced [Ca<sup>2+</sup>]<sub>i</sub> signals. Mean ± SEM, n = 24 - 32 replicates/concentration. IC<sub>50</sub> = 12.1 µM.

### 3 References

- Acuna-Castillo C, et al. 2007. Differential role of extracellular histidines in copper, zinc, magnesium and proton modulation of the P2X7 purinergic receptor. *J Neurochem* 101:17–26.
- Khakh BS, et al. 2001. International union of pharmacology. XXIV. Current status of the nomenclature and properties of P2X receptors and their subunits. *Pharmacol Rev* 3:107-118.
- North RA. 2002. Molecular physiology of P2X receptors. *Physiol Rev* 82:1013-1067.
- Stokes L, et al. 2006. Characterization of a selective and potent antagonist of human P2X7 receptors, AZ11645373. *Br J Pharmacol* 149: 880–887.